Effects of Bistatic Operation in Harmonic Radar

Anastasia Lavrenko
Faculty of Electrical Engineering. Mathematics and Computer Science
University of Twente, the Netherlands
a.lavrenko@utwente.nl

***Abstract*— Harmonic radar systems are used to interrogate, or track a location of, passive nonlinear targets in highly cluttered environments, and they are notorious for their poor power efficiency and low detection ranges. Due to harmonic operation, the received signal power close to maximum range becomes inversely proportional to the fourth power of the forward distance (from the radar transmitter to the harmonic target), compared against the inverse second power law for the return distance (from the harmonic target back to the radar receiver). This difference provides additional degrees of freedom for system design when a harmonic radar transmitter and receiver can be positioned at different distances to the target. This paper investigates the effect this has on detection range in harmonic radar.**

***Keywords*— harmonic radar, harmonic tags, bistatic range.**

I. Introduction

Harmonic radar (HR) is a type of nonlinear radar used to interrogate, or track a location of, a simple nonlinear target [1]. It is commonly used in applications where conventional (linear) radar is ineffective due to background clutter. Most prominent examples include tracking of small wildlife such as insects and small invertebrates [2], [3], search and rescue [4], and detection of electronic devices [5].

In classical radar, the radar transmitter emits a radio frequency (RF) pulse at frequency $f_\mathrm{f} = f_0$ and the radar receiver listens for reflections from a passive target at the same frequency. In contrast, a HR target is nonlinear, so its response is rich in harmonics. Among these, the second harmonic is usually the strongest so that the HR receiver is tuned to $f_\mathrm{h} = 2f_0$. This basic operation is schematically illustrated in Figure 1. Often, such a harmonic response is induced by attaching a battery-less harmonic transponder tag to the target of interest. HR tags typically combine a resonant antenna, a low-voltage diode and possibly a simple impedance matching network. An example of such a harmonic tag operating at a fundamental carrier frequency of $f_\mathrm{f} = 2.9$ GHz and a harmonic return frequency of $f_\mathrm{h} = 5.8$ GHz is shown in Fig. 2 [6]. The main advantage of HR is that the background clutter is greatly reduced, since RF reflection from most objects is linear and stays at f_f.

Due to harmonic operation, the signal power in the forward link (from the HR transmitter to the harmonic tag) becomes inversely proportional to the fourth power of the distance, compared to the inverse second power law in the return link (from the harmonic target to the HR receiver). This difference in path loss between the forward and return links is unique to harmonic radar and it provides an additional degree of freedom for system design. It allows a forward/return range trade-off

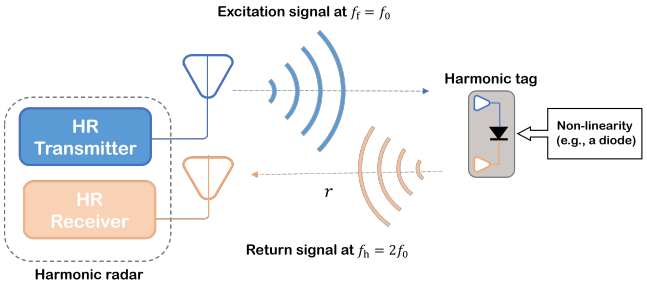

Fig. 1. Harmonic radar principle: a nonlinear harmonic tag is illuminated with an RF signal at a fundamental carrier frequency $f_\mathrm{f} = f_0$ and produces a signal return at $f_\mathrm{h} = 2f_0$.

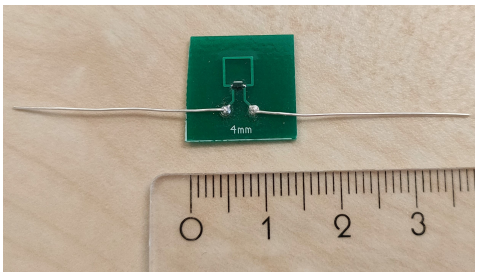

Fig. 2. Harmonic tag with a half-wavelength wire dipole antenna and a printed inductive loop operating at a fundamental carrier frequency of $f_\mathrm{f} = 2.9$ GHz and a harmonic return frequency of $f_\mathrm{h} = 5.8$ GHz [6].

in a bistatic setup when the HR transmitter and receiver can be positioned at different distances to the target. This paper investigates the effect such a bistatic operation has on detection range in harmonic radar. It demonstrates that placing a HR receiver and transmitter at different distances to the target allows an extension of the total bistatic range, as well as a greater forward/return range. To the best of our knowledge, this unique property of HR has not been addressed so far. In a practical system, it can be used to increase system's coverage, or signal-to-noise ratio (SNR), e.g., by having a HR transmitter and a receiver placed on a mobile platform such as UAVs for instance [7].

II. Harmonic radar

A. Monostatic operation

Consider a monostatic HR operation where HR transmitter and receiver are collocated and both are positioned at a distance r from the tag, as shown in Fig. 1. Suppose that the harmonic radar transmitter has a total transmit power of P_t and a transmit

antenna gain G_t. Then, the power density incident on the tag is

$$S_\mathrm{i} = \frac{P_\mathrm{t} G_\mathrm{t}}{4\pi r^2}, \tag{1}$$

while its total received power is $P_\mathrm{i} = S_i A_\mathrm{e,tag}$, where $A_\mathrm{e,tag}$ is the effective aperture of the tag antenna at f_f. The latter is related to the tag antenna gain at f_f, $G_\mathrm{tag}(f_\mathrm{f})$, as

$$A_\mathrm{e,tag} = \frac{G_\mathrm{tag}(f_\mathrm{f})\lambda_\mathrm{f}^2}{4\pi}, \tag{2}$$

where $\lambda_\mathrm{f} = c/f_\mathrm{f}$ is the wavelength and c is the speed of light. With the help of (2), one obtains the following expression for the received power at the tag

$$P_\mathrm{i} = \frac{P_\mathrm{t} G_\mathrm{t}}{(4\pi r)^2} G_\mathrm{tag}(f_\mathrm{f})\lambda_\mathrm{f}^2. \tag{3}$$

The amount of power re-radiated by the tag at f_h is then $P_\mathrm{o} = \eta P_\mathrm{i}$, where η is the power conversion efficiency of the tag, whereas the power received back at the harmonic radar is given by

$$P_\mathrm{r} = S_\mathrm{r} A_\mathrm{e,r} = \frac{P_\mathrm{o} G_\mathrm{r}}{(4\pi r)^2} G_\mathrm{tag}(f_\mathrm{h})\lambda_\mathrm{h}^2, \tag{4}$$

where $S_\mathrm{r} = P_\mathrm{o} G_\mathrm{tag}(f_\mathrm{h})/4\pi r^2$ is the incident received power density and $A_\mathrm{e,r} = G_\mathrm{r}\lambda_\mathrm{h}^2/4\pi$ is the effective aperture of the receive antenna that operates at f_h. Substituting (3) and P_o into (4), the following harmonic radar equation can be obtained

$$P_\mathrm{r} = \frac{P_\mathrm{t} G_\mathrm{t} G_\mathrm{r}}{(4\pi)^3 r^4}\lambda_\mathrm{f}^2 \eta \underbrace{\frac{G_\mathrm{tag}(f_\mathrm{f}) G_\mathrm{tag}(f_\mathrm{h})\lambda_\mathrm{h}^2}{4\pi}}_{\sigma} = \frac{P_\mathrm{t} G_\mathrm{t} G_\mathrm{r}}{(4\pi)^3}\frac{\lambda_\mathrm{f}^2}{r^4}\eta\sigma, \tag{5}$$

where, by analogy with conventional radar systems, $\eta\sigma = \eta G_\mathrm{tag}(f_\mathrm{f}) G_\mathrm{tag}(f_\mathrm{h})\lambda_\mathrm{h}^2/4\pi$ can be viewed as a radar cross-section (RCS) of the harmonic tag.

It turns out that (5) is only valid for large incident power levels and it fails to describe tag behaviour at the maximum range when P_i is low. The reason behind this is the non-linear nature of the tags – their conversion efficiency depends on the incident power level. Figure 3 demonstrates this by showing conversion efficiency of a zero-bias Schottky diode SMS7630-040 commonly used in harmonic tags. It shows that at lower excitation levels, linear relationship between the input and output power does not hold anymore. Instead, there are two clearly distinguishable operation regions [8]:

1) (quasi)-linear region where $\eta \approx$ const and, similar to conventional (linear) radar,

$$P_\mathrm{r} \propto \frac{1}{r^4}; \tag{6}$$

2) (quasi)-quadratic region where $\eta \approx P_\mathrm{o}/P_\mathrm{i} = kP_\mathrm{i}$ in which k is a constant that has units of Watt^{-1}, when

$$P_\mathrm{r} \propto \frac{1}{r^6}. \tag{7}$$

This indicates that at low excitation levels that are characteristic of the tag operation close to maximum range, the received signal power is inversely proportional to the sixth power of the distance, in contrast to the fourth power-law in classical radar. As a result, the received power in harmonic radar decays much faster with distance than in linear radar. Taking into account that $\eta = P_\mathrm{o}/P_\mathrm{i} = kP_\mathrm{i}$ close to maximum range, (5) can be re-written as

$$P_\mathrm{r} = \frac{P_\mathrm{t}^2 G_\mathrm{t}^2 G_\mathrm{r}}{(4\pi)^5}\frac{\lambda_\mathrm{f}^4}{r^6} G_\mathrm{tag}(f_\mathrm{f}) k\sigma, \tag{8}$$

which becomes the harmonic radar equation at the maximum range. Suppose now $P_\mathrm{r,min}$ denotes the receiver sensitivity (i.e., the minimum received power required for reliable signal detection). The corresponding maximum detectable range r_max can then be derived from (8) to be

$$r_\mathrm{max} = \sqrt[6]{\frac{P_\mathrm{t}^2}{P_\mathrm{r,min}} G \frac{\lambda_\mathrm{f}^4}{(4\pi)^5} k\sigma}, \tag{9}$$

where $G = G_\mathrm{t}^2 G_\mathrm{r} G_\mathrm{tag}(f_\mathrm{f})$. Expression (9) thus represents a range equation for monostatic harmonic radar.

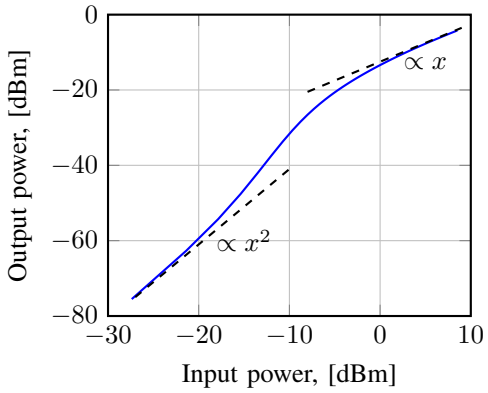

Fig. 3. Simulated conversion efficiency of a zero-bias Schottky diode SMS7630-040 at the fundamental carrier frequency $f_\mathrm{f} = 2.9$GHz and the harmonic return frequency $f_\mathrm{h} = 5.8$GHz.

B. Bistatic operation

All analysis until now assumed monostatic operation in which the HR transmitter and receiver are collocated and the round-trip distance is $2r$. Consider now a bistatic case where the HR transmitter and receiver are located at different distances to the tag so that the round-trip distance is $r_1 + r_2$ where r_1 and r_2 are the forward (HR transmitter-tag) and return (HR receiver-tag) distances, respectively. Due to the squaring action of the tag close to the maximum range (i.e., $\eta = kP_\mathrm{i}$), the power received back at HR receiver becomes inversely proportional to the fourth power of the forward distance. As a result, the bistatic harmonic range equation becomes

$$\sqrt[3]{r_\mathrm{1,max}^2 r_\mathrm{2,max}} = \sqrt[6]{\frac{P_\mathrm{t}^2}{P_\mathrm{r,min}} G \frac{\lambda_\mathrm{f}^4}{(4\pi)^5} k\sigma}. \tag{10}$$

where $r_\mathrm{1,max}, r_\mathrm{2,max}$ denote the maximum forward and return bistatic ranges, respectively.

From (10) and (9), it becomes clear that the following relationship between the bistatic and monostatic ranges should hold

$$r_\mathrm{1,max}^2 r_\mathrm{2,max} = r_\mathrm{max}^3. \tag{11}$$

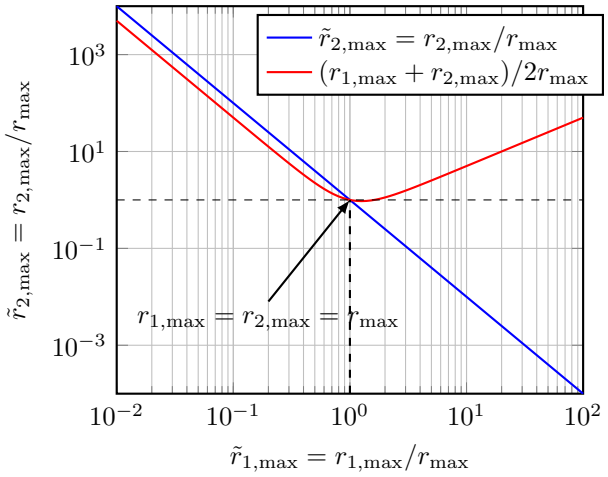

Fig. 4. Relation between maximum bistatic ($r_{1,\max}, r_{2,\max}$) and monostatic ($r_{\max}$) ranges in a harmonic radar system.

Introducing normalized bistatic ranges $\tilde{r}_{1,\max} = r_{1,\max}/r_{\max}$, $\tilde{r}_{2,\max} = r_{2,\max}/r_{\max}$, (11) becomes

$$\tilde{r}_{1,\max}^2 \tilde{r}_{2,\max} = 1. \tag{12}$$

Expression (12) outlines the main trade-off of the bistatic configuration in harmonic radar: for a fixed maximum forward distance $r_{1,\max}$, maximum return distance is $r_{2,\max} = 1/r_{1,\max}^2$, whereas for a fixed maximum return distance $r_{2,\max}$ one obtains $r_{1,\max} = 1/\sqrt{r_{2,\max}}$. Fig. 4 quantifies the degrees of freedom this provides by showing $\tilde{r}_{2,\max}$ as a function of $\tilde{r}_{1,\max}$. For comparison, it also shows the total resulting round-trip range of a bistatic system $r_{1,\max} + r_{2,\max}$ normalized to the total round-trip range of the monostatic system $2r_{\max}$. Fig. 4 demonstrates that the maximum bistatic range is always greater or equal to the maximum monostatic range and that ten-fold reduction of the the forward distance allows a hundred-fold increase of the return one.

III. Experimental Evaluation

This section evaluates the properties of bistatic operation in harmonic radar on an example of a system operating in the S-band with $f_\mathrm{f} = 2.9$ GHz and $f_\mathrm{h} = 5.8$ GHz. For producing a harmonic response, a harmonic tag from [6] was used. It consists of a single wire dipole antenna, a Skyworks Schottky diode SMS7630-040 and a parallel inductive loop, as shown in Figure 2. The dipole length was set to $\ell = 5.8$cm which constitutes $0.56\lambda_\mathrm{f}$. The tag response was measured in an anechoic chamber using a spectrum analyser tuned to f_h and a signal generator as a transmitter producing an illuminating tone signal at f_f. To emulate bistatic operation, transmit and receive antennas were positioned at different distances to the tag, as schematically illustrated in Figure 5.

First set of measurements was performed in a monostatic configuration where $r_1 = r_2 = r$ and the maximum range is described by (10). In this case, (10) predicts that, all other

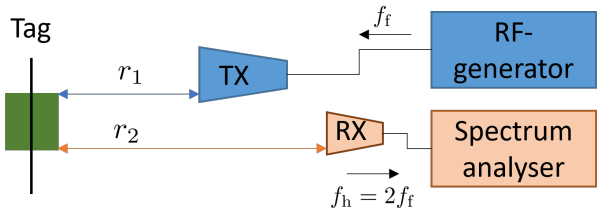

Fig. 5. Schematic illustration of the measurement setup.

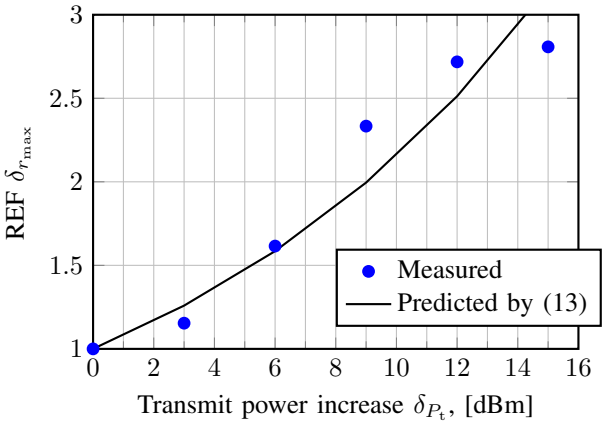

Fig. 6. REF as a function of transmit power increase in a monostatic case.

things being equal, an increase in transmit power by δ_{P_t} should lead to a range extension factor (REF) of

$$\delta_{r_{\max}} = \frac{\sqrt[6]{\frac{P_\mathrm{t}^2 \delta_{P_\mathrm{t}}^2}{P_{\mathrm{r,min}}} G \frac{\lambda_\mathrm{f}^4}{(4\pi)^5} k\sigma}}{\sqrt[6]{\frac{P_\mathrm{t}^2}{P_{\mathrm{r,min}}} G \frac{\lambda_\mathrm{f}^4}{(4\pi)^5} k\sigma}} = \sqrt[3]{\delta_{P_\mathrm{t}}}. \tag{13}$$

Figure 6 shows a comparison between an experimental REF and a theoretical one computed according to (13). The former was evaluated by changing transmit power at the signal generator and measuring the corresponding detection range as the maximum distance r at which the return signal was still detectable above the noise level. One can observe that measurement results align remarkably well with the theoretically predicted curve.

Next, a bistatic configuration was evaluated for different combinations of forward, r_1, and return, r_2, distances. In this case, transmit power was fixed and the two distances were varied by independently changing the position of the transmit/receive antennas with respect to the tag, as indicated in Figure 5. Since measuring maximum ranges in this case was impractical, the values of the received signal power as a function of r_1, r_2 were recorded instead. Although this doesn't allow direct measurement of the maximum bistatic ranges, one can use the fact that as long as the tag is in the (quasi)-quadratic region and all the rest of the parameters besides the distances are equal, for (11) to hold the following relationship should hold as well

$$\sqrt[6]{\frac{P_\mathrm{r}^\mathrm{m}}{P_\mathrm{r}^\mathrm{b}}} = \frac{\sqrt[3]{r_1^2 r_2}}{r} = \frac{R}{r}, \tag{14}$$

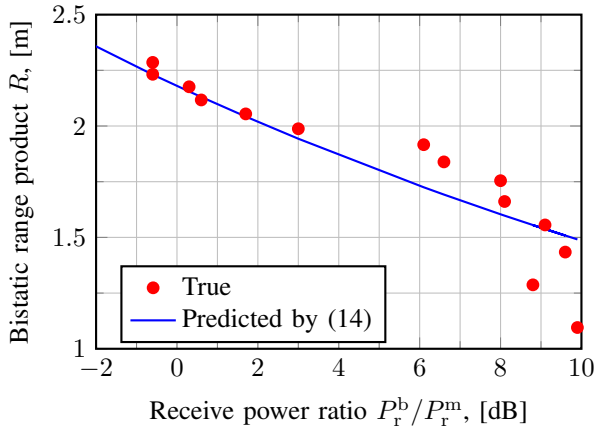

(a) Forward distance fixed at $r_1 = 1.08r$

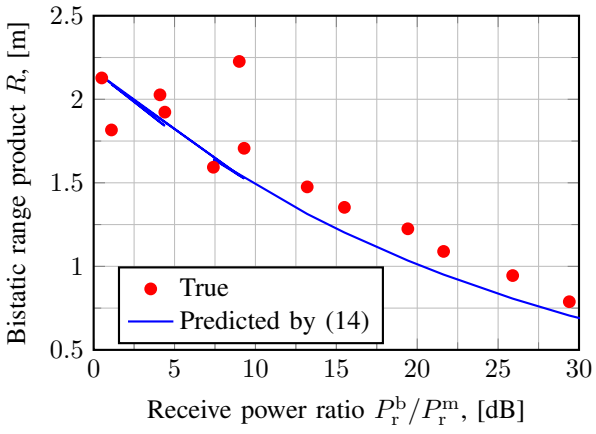

(b) Return distance fixed at $r_2 = r$

Fig. 7. Recorded and predicted by (14) bistatic range $R = \sqrt[3]{r_1^2 r_2}$ as a function of the received signal power ratio $P_{\mathrm{r}}^{\mathrm{b}}/P_{\mathrm{r}}^{\mathrm{m}}$ for (a) fixed value of r_1 and a variable r_2 and (b) fixed value of r_2 and a variable r_1.

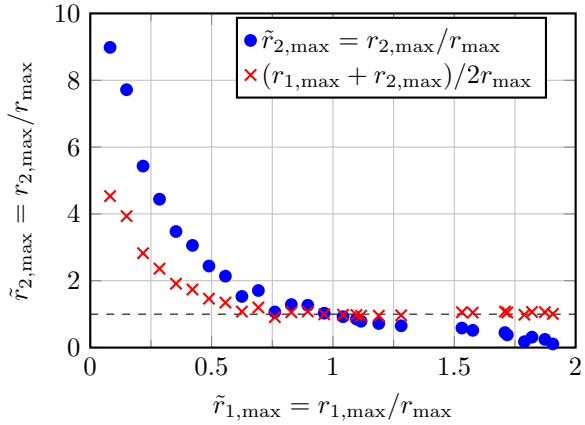

Fig. 8. Relation between maximum estimated bistatic $(r_{1,\max}, r_{2,\max})$ and monostatic $(r_{\max})$ ranges.

where $P_{\mathrm{r}}^{\mathrm{b}}$, $P_{\mathrm{r}}^{\mathrm{m}}$ denote received signal power in the bistatic and monostatic configuration, respectively, r_1, r_2, r are the corresponding distances and $R = \sqrt[3]{r_1^2 r_2}$ is the bistatic range product. Figure 7 investigates how well (14) holds by comparing the true recorded value of the bistatic range R to the one predicted by (14) from the measurements of $P_{\mathrm{r}}^{\mathrm{m}}, P_{\mathrm{r}}^{\mathrm{b}}$, and r. It shows the results for two cases: when r_1 is fixed while r_2 varied (Figure 7a) and vice versa (Figure 7b). Recorded and theoretically predicted values follow each other reasonably well, which suggests that both (10) and (11) provide adequate description of the tag operation in bistatic case.

Finally, from the measurements of $P_{\mathrm{r,min}}$ and $P_{\mathrm{r}}^{\mathrm{b}}$ one can also make an indirect estimation of the maximum bistatic ranges, since for any fixed range product $R = r_1^2 r_2$, one obtains

$$\sqrt[3]{\frac{R}{r_{1,\max}^2 r_{2,\max}}} = \sqrt[6]{\frac{P_{\mathrm{r,min}}}{P_{\mathrm{r}}^{\mathrm{b}}}}. \tag{15}$$

This allows calculation of the maximum forward (return) bistatic range from the given return (forward) range and the power difference between $P_{\mathrm{r}}^{\mathrm{b}}$ and $P_{\mathrm{r,min}}$. Figure 8 shows the combined result for both cases (i.e., fixed forward and fixed return distances). It shows a remarkably similar trend as the one predicted by Figure 4.

IV. Conclusion

This paper studies effects of bistatic operation on detection range in harmonic radar. Presented analysis suggests that by using a bistatic setup one can not only increase the total operational range of a harmonic radar system compared to a monostatic configuration but also significantly increase the return distance by reducing the forward distance, or vice versa.

Acknowledgment

The author would like to thank S. Kolkman and S. Sharma for their assistance during measurements.

References

[1] A. Mishra and C. Li, "A review: Recent progress in the design and development of nonlinear radars," *Remote Sensing*, vol. 13, no. 24, p. 4982, 2021.

[2] W. Daniel Kissling, D. E. Pattemore, and M. Hagen, "Challenges and prospects in the telemetry of insects," *Biological Reviews*, vol. 89, no. 3, pp. 511–530, 2014.

[3] M. E. O'Neal, D. Landis, E. Rothwell, L. Kempel, and D. Reinhard, "Tracking insects with harmonic radar: a case study," *American Entomologist*, vol. 50, no. 4, pp. 212–218, 2004.

[4] T. Harzheim, M. Mühmel, and H. Heuermann, "A SFCW harmonic radar system for maritime search and rescue using passive and active tags," *International Journal of Microwave and Wireless Technologies*, vol. 13, no. 7, pp. 691–707, 2021.

[5] G. J. Mazzaro, A. F. Martone, K. I. Ranney, and R. M. Narayanan, "Nonlinear radar for finding RF electronics: System design and recent advancements," *IEEE Transactions on Microwave Theory and Techniques*, vol. 65, no. 5, pp. 1716–1726, 2017.

[6] A. Lavrenko, B. Litchfield, G. Woodward, and S. Pawson, "Design and evaluation of a compact harmonic transponder for insect tracking," *IEEE Microwave and Wireless Components Letters*, vol. 30, no. 4, pp. 445–448, 2020.

[7] A. Lavrenko, Z. Barry, R. Norman, C. Frazer, Y. Ma, G. Woodward, and S. Pawson, "Autonomous swarm of UAVs for tracking of flying insects with harmonic radar," in *93rd Vehicular Technology Conference (VTC2021-Spring)*, 2021, pp. 1–5.

[8] A. Lavrenko and J. Cavers, "Two-region model for harmonic radar transponders," *Electronics Letters*, vol. 56, no. 16, pp. 835–838, 2020.